Motion of vortex pairs in the ferromagnetic and antiferromagnetic anisotropic Heisenberg model

A. R. Völkel, F. G. Mertens,* A. R. Bishop, and G. M. Wysin†

*Theoretical Division and Center for Nonlinear Studies, Los Alamos National Laboratory,
Los Alamos, New Mexico 87545*

We study the motion of a pair of unbound vortices in two-dimensional classical spin systems with easy-plane exchange symmetry (XY symmetry). Assuming a velocity-independent shape we derive an equation of motion for one vortex in the presence of the other. The results are compared with a direct molecular-dynamics simulation on a 50×50 square lattice at zero temperature. For both the ferromagnet and the antiferromagnet there exists a critical value λ_c of the anisotropy parameter λ which separates two regimes with different stable vortex structures. For $\lambda < \lambda_c$ the spins creating a vortex are essentially in the easy plane and the motion of a pair of vortices is mainly determined by repulsive or attractive forces for equal or different vorticities, respectively. For $\lambda > \lambda_c$ the vortices have additional out-of-plane spin components which depend on λ. In the ferromagnetic case these z components are parallel to each other and act effectively on the other vortex like a magnetic field. Together with the attraction or repulsion discussed above, this effective field leads to rotation of the vortices around each other, or to a translation parallel to each other, depending on whether the products of the vorticity and the sign of the out-of-plane components are equal or different for the two vortices. For an antiferromagnetic out-of-plane vortex, however, the z components of the spins are antialigned and therefore do not give an effective magnetic field, here the vortices move essentially on straight lines. In our simulations we observe the above discussed trajectories. The fluctuations around these trajectories due to the discreteness of the lattice are more pronounced for $\lambda < \lambda_c$ than for $\lambda > \lambda_c$.

I. INTRODUCTION

In many areas of condensed-matter physics and materials science, it is important to understand the relationship between microscopic (atomistic) and macroscopic properties. This connection between underlying elementary interactions and macroscopic responses often rests on the structure, dynamics, and interactions between collective, coherent excitations of an intermediate ("mesoscopic") scale. In nonlinear systems these collective excitations include not only spatially extended modes such as spin waves or phonons, but also spatially local structures such as dislocations or vortices, which may have quasiparticle-like characteristics. It is then important to develop phenomenological theories based on the collective variables—these theories approximate the complete many-particle description in terms of a tractably small number of dominant modes.

The recent heightened interest in quasi-two-dimensional magnetic materials has provided opportunities to apply the above approach. Here the underlying Hamiltonian may take the form of spins with Heisenberg interactions and Landau dynamics, and collective excitations may be, e.g., vortices, domain walls, and spin waves. Inelastic neutron scattering allows measurements of dynamic structure functions.

Examples from the rapidly growing class of quasi-two-dimensional magnetic materials are (1) layered magnets,[1] like K_2CuF_4, Rb_2CrCl_4, $(CH_3NH_3)_2CuCl_4$, and $BaM_2(XO_4)_2$ with $M=$Co,Ni,... and $X=$As,P,...; (2) $CoCl_2$ graphite intercalation compounds;[2] (3) magnetic

lipid layers,[3] like $Mn(C_{18}H_{35}O_2)_2$; here even monolayers can be produced, which are literally two dimensional as concerns their magnetic properties. The above materials fall basically into XY or "easy-plane" symmetry, described by the anisotropic Heisenberg Hamiltonian

$$H = -J \sum_{\langle mn \rangle} (S_m^x S_n^x + S_m^y S_n^y + \lambda S_m^z S_n^z) . \qquad (1.1)$$

Here $\langle m,n \rangle$ label nearest-neighbor sites and (x,y,z) spin components. $J > 0$ and $J < 0$ correspond to ferromagnetic and antiferromagnetic couplings, respectively, and $0 \le \lambda < 1$ for XY spin symmetry.

The XY symmetry leads to a well-known topological phase transition[4] at a temperature T_{KT} (the Kosterlitz-Thouless transition). Below T_{KT}, vortex-antivortex spin configurations appear as thermal excitations in bound pairs; for $T > T_{KT}$, these bound states dissociate and the density of unbound vortices increases with T. At sufficiently high T, the mean spacing between unbound vortices approaches the vortex core size and diffusive spin dynamics results. However, close to T_{KT}, the unbound vortex density is small enough that a phenomenology built on weakly interacting vortices moving ballistically between interactions is possible. A model of dynamics built on such a "vortex gas" has been constructed,[5] assuming a Gaussian velocity distribution from vortex-vortex random interactions. This model suggests a vortex contribution to dynamical spin correlations in the form of a "central peak," i.e., scattering intensity centered at zero frequency. Central-peak scattering calculated in a vortex phenomenology for $T \gtrsim T_{KT}$ has been satis-

factorily compared with a combined Monte Carlo molecular-dynamics simulation for both ferromagnetic[5,6] and antiferromagnetic[7] models [Eq. (1.1)]. Here Landau-Lifshitz dynamics is assumed, viz.,

$$\frac{d\mathbf{S}}{dt} = [\mathbf{S}, H] \ . \tag{1.2}$$

Our aim here is to derive effective equations of motion for the collective (center-of-mass) vortex variables and to test predictions of vortex-vortex and vortex-antivortex interactions against molecular-dynamics simulations of the full spin system. Vortex equations of motion follow the general procedure suggested for magnetic systems by Thiele,[8] Huber,[9] and Pokrovsky, Feigl'man, and Tsvelick.[10] Namely, vortex solutions of (1.1) are used to motivate an ansatz spin profile which is substituted in (1.2) and allowed to evolve under constraints of a finite number of collective variables: For simplicity we restrict our discussion here to a center-of-mass variable, excluding additional shape variations. We consider only a square lattice and we include damping terms in Eq. (1.2).

There is some similarity here to vortex dynamics in other contexts, including incompressible fluid flows,[11] flux lines in superconductors,[12] and vortices in superfluids.[13] However, there are important differences. First, the spin model (1.1) is on a discrete lattice: This leads to lattice pinning effects in certain situations which can dominate vortex-vortex interactions. Second, the spin system contains variables S^x and S^y, in which the vortex singularity resides, but also an out-of-plane component S^z: Importantly, this leads to two types of stable vortex structures, depending on λ, with distinct dynamics. For $\lambda < \lambda_c$ (≈ 0.72 on a square lattice) static vortices are purely in-plane; for $\lambda > \lambda_c$ an additional out-of-plane component develops: The size of this S^z component increases with λ, allowing a continuous crossover to the isotropic Heisenberg limit ($\lambda = 1$), where the topological excitations are merons and instantons[14] rather than vortices. Thus, for $\lambda > \lambda_c$, vortices are characterized by two "quantum numbers": q, the vorticity (i.e., vortex or antivortex), and p, the sign of the out-of-plane component. As we show below, the interaction between two vortices depends on both p and q and can result in either parallel motion or mutual rotation. For $\lambda < \lambda_c$, vortex motion is dominated by attractive or repulsive forces along the connection line.

The structure of the remaining sections is as follows. In Sec. II we derive effective equations of motion for in- and out-of-plane ferromagnetic vortices and pair interactions. In Sec. III those predictions are compared with direct molecular-dynamics simulations. In Sec. IV these results are extended to the antiferromagnetic case by introducing two sublattice spin variables. In this case it is found that vortex-vortex interactions are purely attractive or repulsive along straight lines for all λ. Section V contains a short summary.

II. PAIR INTERACTIONS OF FERROMAGNETIC VORTICES: THEORY

A. Equation of motion for a single vortex

A theory which describes the motion of localized excitations in classical magnetic systems was first developed

by Thiele,[8] who explicitly considered domain walls. Based on this approach, Huber[9] and Pokrovsky, Feigl'man, and Tsvelick[10] made similar calculations for the motion of vortices. In XY-symmetry magnetic systems, the vortices occur in two different phases: In the low-temperature phase there exist pairs, each consisting of two vortices with different vorticities which start to dissociate above the Kosterlitz-Thouless transition temperature T_{KT}. Just above T_{KT} there are only a few free vortices which can be treated as an ideal gas of particles with an average distance 2ξ, where ξ is the correlation length.

In this paper we consider the motion of free vortices on two-dimensional anisotropic Heisenberg systems with ferromagnetic or antiferromagnetic nearest-neighbor exchange interactions. The dynamics of these kinds of systems is described by the Landau-Lifshitz-Gilbert equation

$$\frac{d\mathbf{M}_n}{dt} = -\gamma \mathbf{M}_n \times \frac{\delta w}{\delta \mathbf{M}_n} + \alpha \frac{d\mathbf{M}_n}{dt} \times \frac{\mathbf{M}_n}{|\mathbf{M}_n|} \ , \tag{2.1}$$

where $\mathbf{M}_n$ is the magnetization vector and is proportional to the spin $\mathbf{S}_n$, and w is the energy [given by Eq. (1.1)] per unit volume. The parameter α describes in a phenomenological way the damping of the motion of the vortices due to spin fluctuations. For the subsequent calculations we consider vortices with a fixed shape and, following the ideas of Thiele,[8] we obtain an equation for the average velocity of a single vortex in the continuum limit:

$$\mathbf{G} \times \mathbf{v} + \mathbf{D} \cdot \mathbf{v} + \frac{\gamma}{m_0} \mathbf{F} = 0 \ . \tag{2.2}$$

With the magnetization field $\mathbf{M}$ expressed in terms of the spherical coordinates $\phi(\mathbf{r})$ and $\theta(\mathbf{r})$, which describe the in- and out-of-plane structures, respectively, the gyrovector $\mathbf{G}$ and the dissipation matrix D are defined by

$$\mathbf{G} = \int d^2r \, \sin\theta(\mathbf{r}) \mathrm{grad}\theta(\mathbf{r}) \times \mathrm{grad}\phi(\mathbf{r}) \ , \tag{2.3}$$

and

$$D_{kl} = -\alpha \int d^2r \, [\nabla_k \theta(\mathbf{r}) \nabla_l \theta(\mathbf{r}) \\ + \sin^2\theta(\mathbf{r}) \nabla_k \phi(\mathbf{r}) \nabla_l \phi(\mathbf{r})] \ . \tag{2.4}$$

γ is the gyromagnetic ratio, and m_0 is the local magnetic moment per unit area, which, on a square lattice (lattice constant a) and at low temperatures, has the form[9]

$$m_0 = \frac{\hbar\gamma}{a^2} \ . \tag{2.5}$$

The static force between two vortices is

$$\mathbf{F} = 2\pi J S^2 q_1 q_2 \frac{\mathbf{R}_{12}}{R_{12}^2} \ , \tag{2.6}$$

which was calculated for the planar XY model,[4] but should also be valid for systems with small λ, where the static vortex is purely in-plane (λ describes the coupling between the z components of the spins and has values of $0 \le \lambda < 1$ for our systems). For systems with a λ larger than the critical λ_c, the vortices have a stable static out-

of-plane structure, which is confined to an area of a few lattice constants around the core (2.9). If the distance between the vortices is large, so that their cores do not overlap, they will only be sensitive to the in-plane structure of the other vortex, which should give the same force (2.6) as for $\lambda < \lambda_c$.

If we make the transformation, $\mathbf{M}$ goes to $-\mathbf{M}$, then the first term of Eq. (2.1) becomes positive, and going further in our calculation, the gyrovector also changes its sign. That means that all the motion which is caused by $\mathbf{G}$ changes its direction. In a microscopic picture the magnetization is the sum over all the magnetic moments in the sample, and in a classical system these magnetic moments are caused by moving and/or rotating charges. Thus the sign of $\mathbf{M}$ is determined by the sign of the charge of the particle. The same change of the sign of the first term in (2.1) is obtained if one makes a transformation from time t to $-t$. The solutions of (2.1) therefore remain unchanged if one changes the signs of both the charge and time; they differ if one applies only one of these two transformations.

Though Eq. (2.2) describes the motion of one vortex in the presence of an arbitrary number of other vortices, which produce the force $\mathbf{F}$, we focus in this paper only on pairs of free vortices which should give us already a good understanding of the dynamics of a dilute gas of vortices.

Out-of-plane vortices

To find the excitations in a system described by the Hamiltonian (1.1), we express the spins using spherical coordinates:

$$\mathbf{S}_n = S(\cos\phi_n\cos\theta_n, \sin\phi_n\cos\theta_n, \sin\theta_n) \ . \tag{2.7}$$

For $\lambda > \lambda_c$ we find stable localized solutions with, in the continuum limit, the static form[6]

$$\phi(\mathbf{r}) = q \arctan\frac{y}{x} \ , \tag{2.8}$$

$$\sin\theta(\mathbf{r}) \sim \begin{cases} p\left[1 - \dfrac{c_1 r^2}{2r_v^2}\right] & \text{as } r \to 0 \ , \\ c_2\sqrt{r_v/r}\,e^{-r/r_v} & \text{as } r \to \infty \ , \end{cases} \tag{2.9}$$

$$r_v = \frac{1}{2}\left[\frac{\lambda}{1-\lambda}\right]^{1/2} \ . \tag{2.10}$$

We call these "out-of-plane" vortices due to their nonzero z component. r_v is the radius of the vortex core,[6] and the constants c_1 and c_2 are determined by matching[6] the two asymptotic solutions in Eqs. (2.9) at $r = r_v$. The integer $q = \pm 1, \pm 2, \ldots$ denotes the vorticity, and a vortex with negative q is called an antivortex. In the present paper we only allow values $|q| = 1$, which agree with observations for temperatures $T \gtrsim T_{\mathrm{KT}}$, where we have a dilute gas of vortices and where we can assume that they will follow Eq. (2.2). p is $+1$ if the out-of-plane structure is above the xy plane, and -1 if it is below. The deformation of the shape for a slowly moving vortex is very small[6] and can be neglected for our purposes.

Inserting Eqs. (2.8) and (2.9) in (2.3) gives the gyrovector[9]

$$\mathbf{G} = 2\pi p q\,\mathbf{e}_z \ , \tag{2.11}$$

where $\mathbf{e}_z$ is the unit vector perpendicular to the plane. For the dissipation matrix we find

$$D_{kl} = D_0\delta_{kl} \ ,$$
$$D_0 = -\alpha\left[\pi\ln\frac{L}{r_a} + \text{const}\right] \ , \tag{2.12}$$

where D_0 is increasing with the total radius L of the vortex; r_a is a cutoff of the order of one lattice constant and denotes the lower bound on the range where the continuum approximation is valid. The constant in (2.12) is mainly determined by the out-of-plane structure and is for $r_v \ll L$ much smaller than the logarithmic term.

With (2.11) and (2.12) we obtain from (2.2) an expression for the velocity of one of the two vortices under consideration ($i = 1, 2$):

$$\mathbf{v}_i = \frac{(a^2/\hbar)F}{D_0^2 + G^2}(-D_0\mathbf{e}_{\mathrm{r},i} + G_i\mathbf{e}_{\varphi,i})$$
$$= \frac{fq_1q_2}{r(1+\epsilon^2)}(\epsilon\mathbf{e}_{\mathrm{r},i} + q_ip_i\mathbf{e}_{\varphi,i}) \ , \tag{2.13}$$

with $f = JS^2a^2\hbar^{-1}$, $\epsilon = -D_0/2\pi$, and $\mathbf{e}_{\mathrm{r},i}, \mathbf{e}_{\varphi,i}$ unit vectors parallel and perpendicular to the line connecting the two vortices, respectively. Because of the definition of the force, the unit vectors for vortices 1 and 2 are antiparallel, which means that the r components of the velocities are always pointing in opposite directions. The angular parts of the velocities, however, depend on the products p_iq_i, and so we have two different types of trajectories.

(i) $p_1q_1 = p_2q_2$ (or, equivalently, $p_1q_2 = p_2q_1$): Here the vortices rotate around each other, while the "center of mass" of both vortices is at rest:

$$\mathbf{v}_{\mathrm{c.m.}} = \frac{\mathbf{v}_1 + \mathbf{v}_2}{2} = 0 \ . \tag{2.14}$$

In the rest frame the velocities have the form

$$\mathbf{v}_i(t) = \frac{(-1)^{1+i}f}{r(1+\epsilon^2)}\{[\epsilon q_1q_2\cos\alpha(t) - p_iq_{3-i}\sin\alpha(t)]\mathbf{e}_{\mathrm{r}_0} + [\epsilon q_1q_2\sin\alpha(t) + p_iq_{3-i}\cos\alpha(t)]\mathbf{e}_{\varphi_0}\} \ , \tag{2.15}$$

with

$$\mathbf{e}_{\varphi_0} = \mathbf{e}_{\varphi,1}(t = 0) \ ,$$
$$\mathbf{e}_{\mathrm{r}_0} = \mathbf{e}_{\mathrm{r},1}(t = 0) \ , \tag{2.16}$$

and we obtain, for the distance between the two vortices

$$r^2(t) = r_0^2 + \frac{2f\epsilon}{1+\epsilon^2}q_1q_2t \ , \tag{2.17}$$

and, for the angle between the two coordinate systems (that is, the angle between the lines which connects the

two vortices at times zero and t),

$$\alpha_i(t) = \alpha_{0,i} + \frac{p_i}{2\epsilon q_i} \ln \left[r_0^2 + \frac{2f\epsilon}{1+\epsilon^2} q_1 q_2 t \right] , \qquad (2.18)$$

where $\alpha_{0,2} = \alpha_{0,1} + \pi$.

(ii) $p_1 q_1 = -p_2 q_2$: For this case the velocity of the "center of mass" has a component perpendicular to the line connecting the two vortices:

$$\mathbf{v}_{\text{c.m.}} = \frac{fp_1 q_2}{r(1+\epsilon^2)} \mathbf{e}_{\varphi,1} . \qquad (2.19)$$

Now the unit vectors $\mathbf{e}_r$ and $\mathbf{e}_\varphi$ are already static and an integration over the r components of the velocities gives the mutual distance as a function of time, which has the same form (2.17) as in case (i). The motion perpendicular to the line connecting the two vortices is described by (2.19) and has the form

$$r_{\text{c.m.}} = \frac{p_1}{\epsilon q_1} \left[\left[r_0^2 + \frac{2f\epsilon}{1+\epsilon^2} q_1 q_2 t \right]^{1/2} - (r_0^2)^{1/2} \right] . \qquad (2.20)$$

The motion in both cases (i) and (ii) can be divided into to different parts. First, the vortices move along their connecting line and the direction is determined by the product of their vorticities (repulsion for equal, attraction for different q's), while the speed is proportional to the damping parameter α. Because of the logarithmic potential between the vortices, which is infinitely extended in two dimensions, a vortex-vortex (or antivortex-antivortex) pair would separate for all times on an infinite lattice. Second, there is also a velocity component perpendicular to their connecting line. Whether these components appear for each vortex in the opposite or in the same direction depends on whether the products of the two numbers q_i and p_i of each vortex are equal ($q_1 p_1 = q_2 p_2$) or not ($q_1 p_1 = -q_2 p_2$), respectively. (Therefore, in a magnetic system the product of the vorticity q and the sign of the out-of-plane component p of a vortex corresponds to the vorticity in the hydrodynamic case.[11]) The sign of the product of the two vorticities $q_1 q_2$ determines the direction of this motion [cf. Eqs. (2.18) and (2.20)].

We also can see that in each of these cases the velocities increase with decreasing distance. Because we performed our analysis in the continuum limit, our results are only valid for distances between the vortices of at least a few lattice constants, where the effects due to the discrete lattice are not so important. In particular, the divergence of the angle α at

$$t_0 = \frac{1+e^2}{2f\epsilon} r_0^2 , \qquad (2.21)$$

for a vortex-antivortex pair, occurs in a range where our theory is not correct—a calculation which deals with the discrete lattice should give a finite α in this range.

C. In-plane vortices

For $\lambda < \lambda_c$ a pure planar vortex is stable in the static case. If this kind of vortex is moving, it develops some additional out-of-plane components so that its structure to first order in the velocity has the form[6] [(r,φ) are the cylindrical coordinates]

$$\phi(\mathbf{r}) = q \arctan \frac{y}{x} , \qquad (2.22)$$

$$\sin\theta(\mathbf{r}) \sim \begin{cases} -\dfrac{v}{JS} r \sin(\varphi - \eta) & \text{as } r \to 0 , \\[2mm] \dfrac{v}{4\delta JS} \dfrac{\sin(\varphi - \eta)}{r} & \text{as } r \to \infty , \end{cases} \qquad (2.23)$$

where η is the angle between the direction of the velocity $\mathbf{v}$ and the x axis, and $\delta = 1 - \lambda$. For $\lambda < \lambda_c$ the vortex core r_v is smaller than one lattice constant, so that the large r limit of $\theta(\mathbf{r})$ can be used in the integrals that give $\mathbf{G}$ and $\mathbf{D}$. We obtain

$$\mathbf{G} = 0 , \qquad (2.24)$$

for the gyrovector because of the φ asymmetry, and

$$D_{kl} = D_1 \delta_{kl} ,$$
$$D_1 = -\alpha \left[\pi \ln \frac{L}{r_a} + \text{const} \right] , \qquad (2.25)$$

for the dissipation dyadic with a different constant than in Eq. (2.12) due to the different out-of-plane structure, but which is also small compared to the logarithmic term for large L. Because of the vanishing gyrovector and the diagonal dissipation matrix, the motion of the vortices in this case is mainly determined by the static force (2.5). This means attraction for $q_1 q_2 < 0$ and repulsion for $q_1 q_2 > 0$, without any velocity component perpendicular to the connecting line (rotation or translation) as in the case $\lambda > \lambda_c$:

$$\mathbf{v} = -\frac{\mathbf{F}}{|D_1|} = \frac{fq_1 q_2}{r|D_1|} \mathbf{e}_r . \qquad (2.26)$$

III. PAIR INTERACTIONS OF FERROMAGNETIC VORTICES: SIMULATIONS

For the numerical simulation we used the Landau-Lifshitz Hamiltonian spin dynamics with Gilbert damping:

$$\frac{d\mathbf{S}_n}{dt} = \mathbf{S}_n \times \mathbf{F}_n - \alpha \mathbf{S}_n \times (\mathbf{S}_n \times \mathbf{F}_n) ,$$
$$\mathbf{F}_n = J \sum_m (S_m^x \mathbf{e}_x + S_m^y \mathbf{e}_y + \lambda S_m^z \mathbf{e}_z) , \qquad (3.1)$$

where m denotes all nearest neighbors of the spin n and α is the damping parameter. In our simulations $\alpha = 0.1$.[15] The increase of α with T does not change the qualitative behavior of our analytical results (Sec. II) in the temperature range under consideration. We considered a 50×50 square lattice with free-boundary conditions. The integration was performed with a fourth-order Runge-Kutta method with time step 0.04 (in units of $\hbar/JS$). For $\lambda < \lambda_c$ we initialized the simulation with two planar vortices, each at the middle of a plaquette of four spins at (x_1, y_1) and (x_2, y_2), respectively: viz.,

$$\phi(\mathbf{r}) = q_1 \arctan\left[\frac{y - y_1}{x - x_1}\right] + q_2 \arctan\left[\frac{y - y_2}{x - x_2}\right] .$$

$$(3.2)$$

When the vortices start moving, they develop out-of-plane components, which have the form (2.23). We also made simulations for $\lambda > \lambda_c$ with the same initial conditions. Here the vortices develop out-of-plane components after some time, described by (2.9), but with "random" p's, depending on numerical effects. To obtain well-defined values for p, we initialized the simulations with a superposition of vortices with different kinds of out-of-plane structures: (i) single static out-of-plane structure and (ii) pure in-plane structure with small z components of the spins surrounding the vortex cores. We obtained the structure of a single out-of-plane vortex by placing an in-plane vortex with a small perturbation in the middle of the lattice and integrating the equations of motion (3.1). Because of the damping, this initial shape relaxes to the in- or out-of-plane structure for $\lambda < \lambda_c$ and $\lambda > \lambda_c$, respectively. For single static vortices on a 50×50 square lattice, we found with this method that $\lambda_c = 0.715 \pm 0.005$. (This value can also be obtained by numerically generating the magnon spectrum in the presence of one in-plane vortex as a function of λ: Above λ_c one of these magnon modes becomes imaginary, corresponding to the change in the vortex structure.[16])

The vortices emit spin waves at all times (especially during the adaptation process), but these excitations are strongly suppressed by the damping—this helps us to identify the vortices more clearly. To determine their positions we used two steps: (i) We searched for all plaquettes with four spins whose total difference in the in-plane angle ϕ is almost $+2\pi$(vortex) or -2π(antivortex); (ii) to estimate the position of the vortex in this plaquette, we used the fact that the difference in ϕ between two adjacent spins is large if the vortex is close to this lattice sites, and vice versa.

While the theory was developed in the continuum limit, the simulation was performed on a discrete, finite lattice. The discreteness effects can be described through a periodic (Peierls-Nabarro) pinning potential.[17] The vortices have minimum energy if their core is in the middle of a plaquette, and they have maximum energy if their core is on a lattice site. The energy difference (Table I) is biggest for $\lambda = 0$, decreases with increasing λ, and is near zero for $\lambda \approx 0.7$.[6] For $\lambda < \lambda_c$ the core has an extension of about one lattice constant, which has the effect that a moving vortex causes big changes in the direction of the spins close to its core—the energy is smallest if the "ferromagnetic order" is less disturbed. In the case $\lambda > \lambda_c$ the out-of-plane structure, which defines the size of the core here, is extended over several lattice sites and the z components of the spins involved are ferromagnetically ordered. Both of these effects give only small changes in the energy while the vortex is moving through the lattice. This behavior, which shows the strong dependence on the underlying lattice, is valid for our classical simulations performed at zero temperature. In a real system, howev-

TABLE I. Energy (in units of JS^2) of a single vortex on a 50×50 lattice for different positions $\mathbf{r}_v$ of the vortex core (in units of the lattice constant).

$\mathbf{r}_v$	Energy
(25.5,25.5)	14.53
(25.5,25.0)	14.81
(25.0,25.0)	15.33

er, we can observe free vortices only above the Kosterlitz-Thouless transition temperature T_{KT}, which has in our system a value ~ 0.8. For $\lambda = 0$ this is of the order of the maximal variation of the energy difference as a function of position on the lattice for a single vortex ($\Delta E \approx 0.8$; see Table I). Therefore, the discreteness effects are negligible in a real system. This is true even for $\lambda = 0$ because the thermal fluctuations are large enough to allow the vortices to overcome all the maxima of the lattice potential. These thermal energy fluctuations are small compared to the vortex energy which is dominated by the contributions of the static structure.[5,6] Only for $\lambda \to 1$ does the static vortex energy become of the order of the thermal and motional energies,[6] consistent with the crossover to isotropic behavior.

There are also strong effects due to the boundaries: In an area of about ten lattice constants along the border line, the vortex dynamics is quite different than in the middle of the system. In some of the simulations (mainly those which we initialized with two single static out-of-plane vortices), we could observe an additional vortex, which was created at one of the edges and which had also some influence on the dynamics of the two vortices under observation.

A. Vortex-vortex simulations (equal q's)

We expect from our analysis above that we have different dynamical scenarios depending on the anisotropy parameter λ. For $\lambda > \lambda_c$ the motion of the vortices mainly depends on their out-of-plane components. Figure 1(a) shows the trajectories of two vortices with equal p's. In this case we have $p_1 q_1 = p_2 q_2$, which means that they rotate around each other. We also expect that vortices with equal q values repel each other, and so we started with a small pair separation in the middle of the lattice, to avoid effects of the boundary for as long as possible:

$$(x_1, y_1) = (23.5, 23.5) ,$$
$$(x_2, y_2) = (24.5, 25.5)$$

$$(3.3)$$

(units in the lattice constant a). The time difference between neighboring points is 12 in our units (this is true for all the ferromagnetic simulations, if not otherwise noted), except for the first six points which are separated by four time units. In Figs. 1(b) and 1(c) we have plotted the velocity and a quantity (qn), which measures the out-of-plane component of the vortices as a function of time, respectively. qn is the average value of the S_z components of the four spins surrounding the vortex core

normalized by S. The velocities have been averaged over four time units, but still show some fluctuations due to the discreteness of the lattice (the vortices move not more than one lattice constant during this time) and errors in calculating the exact position of the vortex center. Even for $\lambda > \lambda_c$ the velocity depends a little on whether the core is moving toward or away from the middle of a plaquette. In Fig. 1(c) we can see that after about 20 time units the vortices adapt from the static out-of-plane structure to their final, stable forms, which have smaller out-of-plane components. The velocity is larger for smaller separations and decreases with time, as expected from (2.17). The small asymmetry of the trajectories for

large t is caused by an additional antivortex created close to (50.0,50.0) and pinned at the boundary.

Figure 2(a) shows the trajectories of a system with the same initial conditions, but with out-of-plane components in different directions. This is a case where $p_1 q_1 = -p_2 q_2$, and we observe that the vortices move in the same direction perpendicular to the connecting line. The rate of increase in the distance is large at the beginning and becomes smaller later. We also see that the perpendicular motion slows down for increasing time. Both behaviors agree with our theoretical results [Eqs. (2.17) and (2.20)].

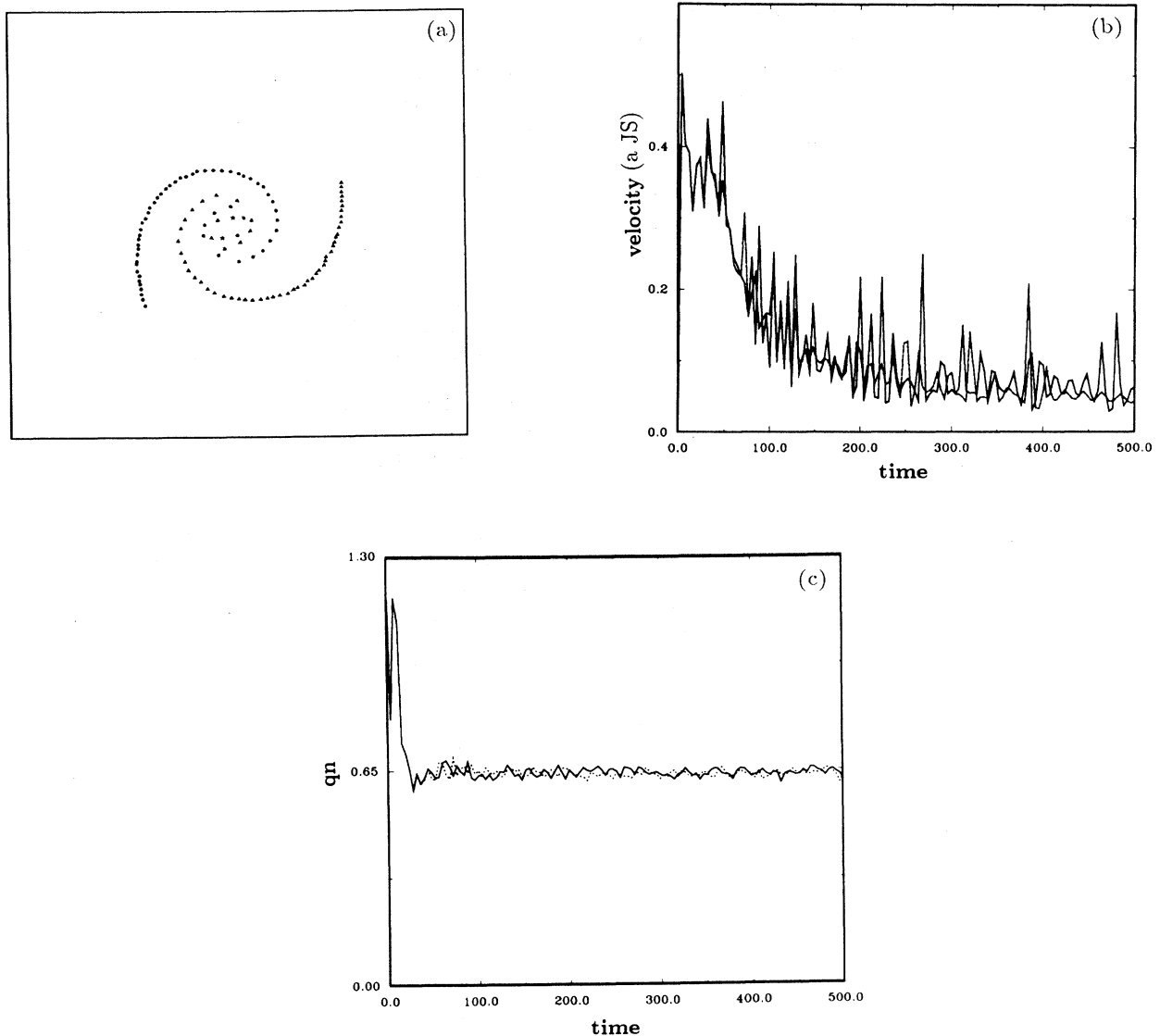For $\lambda < \lambda_c$ the dynamics of the two vortices is quite

FIG. 1. Vortex-vortex simulations on a ferromagnet with $\lambda = 0.9$, $q_1 = q_2 = 1$, $p_1 = p_2 = 1$, and initialized with two static out-of-plane vortices at positions defined in Eq. (3.3): (a) trajectories (star, start positions; circle, vortex 1; triangle, vortex 2); the dashed line is a guide to the eye and connects successive points by straight lines; (b) vortex velocities vs time (solid line, vortex 1; dashed line, vortex 2); (c) out-of-plane components qn [see Sec. III after Eq. (3.3)] vs time; time is measured in units of $(JS)^{-1}$ and qn in units of S.

different, as one can see in Fig. 3. In this case the vortices experience strong lattice effects, which will stop their motion after a relatively short time—the static force between them decreases as r_{12}^{-1} (r_{12} is the mutual separation) and beyond a certain distance is too weak to push them over the walls of the "lattice potential." We also can see that for small λ's the trajectories are almost straight lines and there are only small fluctuations caused by the underlying lattice structure. The theoretical result, which yields motion along straight lines, is only valid in the continuum limit, but for these small λ values the vortex core is of the order of one lattice constant so that this approximation is no longer valid.

The out-of-plane components are due to the velocity (2.23) and increase with increasing velocity and λ. As can be seen from (2.23), all the spins on the left side of the trajectory have negative z components, and all the spins on the other side have positive z components. Hence, along the direction of the motion, the out-of-plane com-
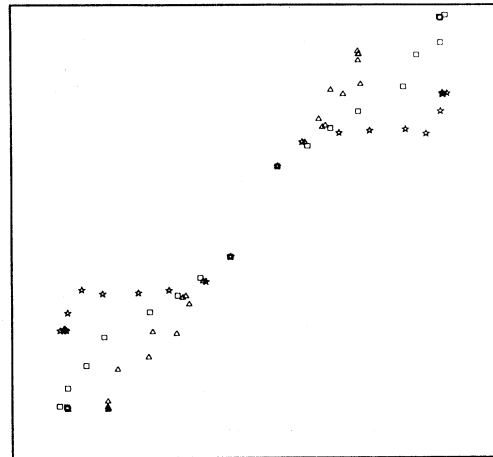

FIG. 3. Trajectories of vortex pairs on a ferromagnet with $\lambda < \lambda_c$ (square, $\lambda = 0.0$; triangle, $\lambda = 0.3$; star, $\lambda = 0.6$), $q_1 = q_2 = 1$, and initialized with two static in-plane vortices. Only a part of the lattice is shown: $18.0 \le x, y, \le 30.0$, and the time between two successive points is four in our units.

ponents of the spins are antiferromagnetic ordered, which is not very favorable for a ferromagnetic system. So, if the spins on this line have a certain z component, depending on λ and v, the out-of-plane vortex, which has a ferromagnetic out-of-plane structure, will have lower energy and will become stable—the vortices will change their shape. This scenario can be seen in Fig. 3 for $\lambda = 0.6$: The initial separation is so small that the velocity that the vortices develop at the beginning is big enough to cause a change in their shape, and they start to rotate around each other due to a nonzero gyrovector. But after a short time the velocity decreases and soon is so small that they become again in-plane vortices. For $\lambda = 0.7$, which is very close to the static critical λ_c, this behavior is even more distinct (Fig. 4): The vortices adapt their shape to

FIG. 2. Same simulation as in Fig. 1, but with $q_1 = -q_2 = 1$: (a) trajectories; (b) qn vs time.
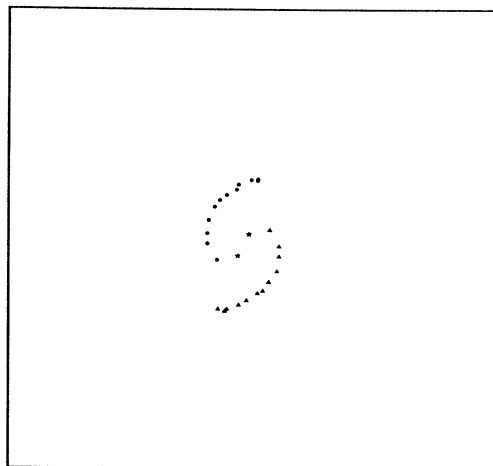

FIG. 4. Trajectories for a vortex pair on a ferromagnet with $\lambda = 0.7$ and initialized with two static in-plane vortices; other parameters as in Fig. 1.

an out-of-plane structure for quite a long time and, be-
cause of their equal p values, rotate around each other.
But eventually the velocity, which is decreasing with
$t^{-1/2}$ (for $t \gg t_0$ and $\lambda > \lambda_c$), is too small and the vortices
will stop as soon as they have changed their shape.

The stability of the in-plane vortex structure also de-
pends on the initial conditions: If we start with two pure
in-plane vortices with equal x or y coordinates, then they
will move on straight lines (along the x or y direction)
even for $\lambda \lesssim \lambda_c$. If we use this kind of initial condition for
a λ, which is bigger than λ_c, then we can see that the in-
plane structure is also stable for quite a long time: about
25 time units for $\lambda = 0.8$ and $(x_1, y_1) = (24.5, 23.5)$,
$(x_2, y_2) = (24.5, 25.5)$ [Figs. 5(a) and 5(b)]. During this
period, the vortices are moving on straight lines, but
finally the out-of-plane structure develops and the dy-
namics of the vortices changes accordingly.

B. Vortex-antivortex simulation (different q's)

If we start with a vortex and an antivortex, they will
attract each other and finally annihilate. To make the
dynamical behavior in this case visible, it is necessary to
start with a bigger initial separation. In our simulation
we chose

$$
\begin{aligned}
(x_1, y_1) &= (21.5, 21.5) \quad \text{(vortex)}, \\
(x_2, y_2) &= (29.5, 30.5) \quad \text{(antivortex)}.
\end{aligned}
\tag{3.4}
$$

Figures 6 and 7 show the trajectories of two vortices in a
system with $\lambda = 0.9$ for equal and different p's, respective-
ly. In Figs. 6(a) and 7(a) we started with a superposition
of two static out-of-plane vortices. Though this seems to
be a good initial condition, for small times we obtain re-
sults that do not agree with our theory, which predicts
for these cases a monotonic decrease of the distance be-
tween the two vortices (2.17). In the simulations, howev-
er, we observe during the first four time units that the
vortices move perpendicular to their initial connecting
line before they increase their mutual distance for about
8–12 time units, and only after these steps do they behave
as theoretically expected. An explanation of this different
behavior is that the initial condition is not sufficient:
Namely, with these two vortices having the "single, static
shape," the system has much more energy than it would
have with two moving vortices, and the process of adapt-
ing to this configuration is responsible for the repulsion at
the beginning of the motion.

In order to avoid this "excess" energy behavior, we
started with two vortices with the pure in-plane struc-
ture, where the four spins around each core had a z com-
ponent of $0.1p$ to guarantee that the out-of-plane struc-
ture of the vortices would develop in the desired direction
($\pm p$). The trajectories for these simulations are shown in
Figs. 6(b) and 7(b) for equal and different p's, respectively.
After a short adaptation process, which occurs within the
first four time units, the vortices indeed move along their
predicted trajectories, viz.: (1) For $p_1 q_1 = -p_2 q_2$ they
move parallel and decrease their separation slowly. Be-
cause our system is too small, we cannot observe the final
annihilation process. (2) For $p_1 q_1 = p_2 q_2$ they rotate and

finally annihilate each other. As one can see from Eq.
(2.18), the rotation angle α is changing faster for smaller
separations between the two vortices.

For $\lambda < \lambda_c$ the vortices move toward each other
without any systematic motion perpendicular to their
connecting line and finally annihilate. However, this can
only happen if the initial separation is small enough, such
that the attraction between them is bigger than the pin-
ning forces due to the lattice.

IV. ANTIFERROMAGNET

If the exchange coupling J in (1.1) is negative, then the
system is an antiferromagnet; i.e., we have two sublattices
with mutual antialigned spins. To calculate the excita-
tions and their dynamics, it is appropriate to parametrize
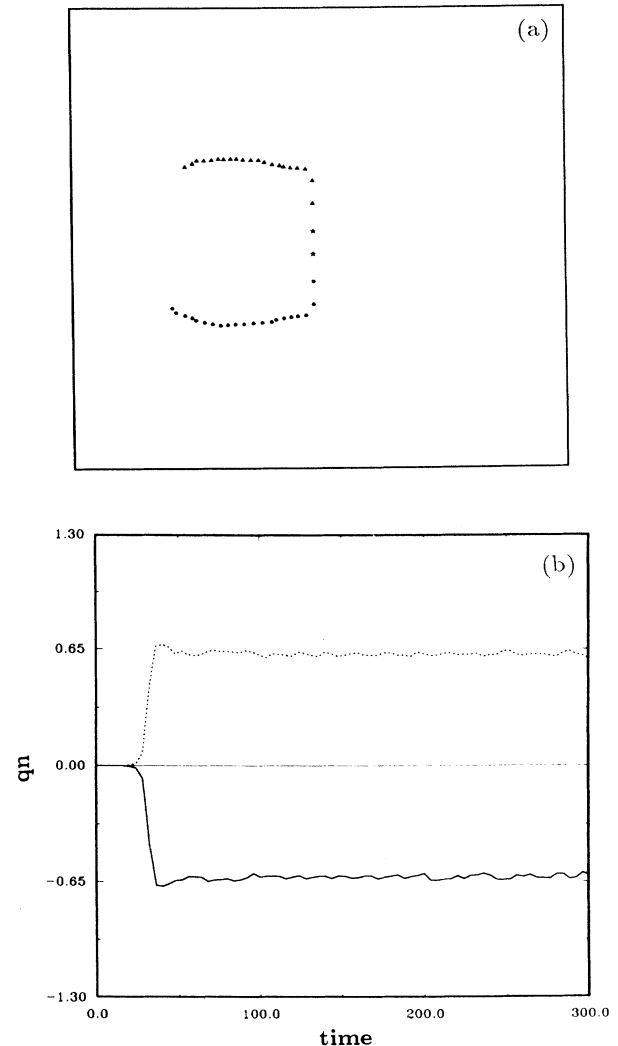the spins by four angles as introduced by Mikeska:[18]

FIG. 5. Same simulation as in Fig. 4, but with $\lambda = 0.8$ and ini-
tial positions $(x_1, y_1) = (24.5, 23.5)$ and $(x_2, y_2) = (24.5, 25.5)$.

$$S_n^x = (-1)^n S \{ \cos[\Phi_n + (-1)^n \phi_n]$$

$$\times \cos[\Theta_n + (-1)^n \theta_n] \} \ ,$$

$$S_n^y = (-1)^n S \{ \sin[\Phi_n + (-1)^n \phi_n]$$

$$\times \cos[\Theta_n + (-1)^n \theta_n] \} \ , \qquad (4.1)$$

$$S_n^z = (-1)^n S \{ \sin[\Theta_n + (-1)^n \theta_n] \} \ ,$$

where the even n describe one sublattice, the odd n the other one. The capital angles describe the perfect antiferromagnetic structure, while the small angles describe the deviations from this state. We are interested here in vortices, and depending on the anisotropy parameter λ, we obtain two stable solutions as in the ferromagnetic case (see Appendix).

(i) $\lambda < \lambda_c$ (in-plane vortices):

$$\Phi(\mathbf{r}) = q \arctan\frac{y}{x}, \quad \phi(\mathbf{r}) = 0, \quad \Theta(\mathbf{r}) = 0 \ ,$$

$$\qquad (4.2)$$

$$\theta(\mathbf{r}) \sim \begin{cases} \dfrac{v}{qJS} r \sin(\varphi - \epsilon) & \text{as } r \to 0 \ , \\[2mm] -\dfrac{v}{4\delta JS} \dfrac{\sin(\varphi - \epsilon)}{r} & \text{as } r \to \infty \ . \end{cases}$$

(ii) $\lambda > \lambda_c$ (out-of-plane vortices):

$$\Phi(\mathbf{r}) = q \arctan\frac{y}{x}, \quad \phi(\mathbf{r}) = f(r,v)\cos(\varphi - \epsilon),$$

$$\Theta(\mathbf{r}) \sim \begin{cases} \pi/2 - c_3 r/r_v & \text{as } r \to 0 \ , \\[2mm] c_4 \sqrt{(r_v/r)}\, e^{-r/r_v} & \text{as } r \to \infty \ , \end{cases} \qquad (4.3)$$

$$\theta(\mathbf{r}) = g(r,v)\sin(\varphi - \epsilon) \ .$$
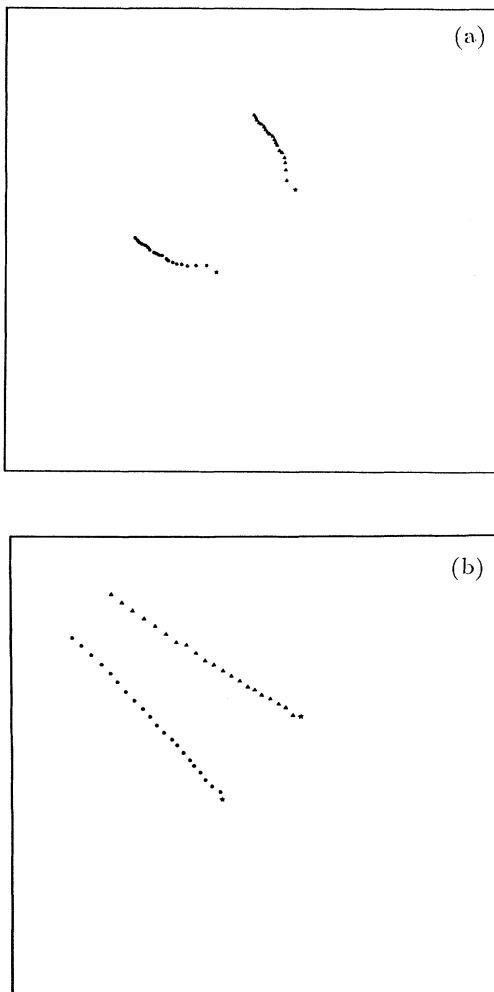
FIG. 6. Trajectories for a vortex-antivortex pair $(q_1 = -q_2 = 1)$ on a ferromagnet with $\lambda = 0.0$ and $p_1 = p_2 = 1$. The initial positions are given by Eq. (3.4) and the initial shapes are (a) static out-of-plane and (b) static in-plane with small perturbations [see Sec. III after Eq. (3.2)].
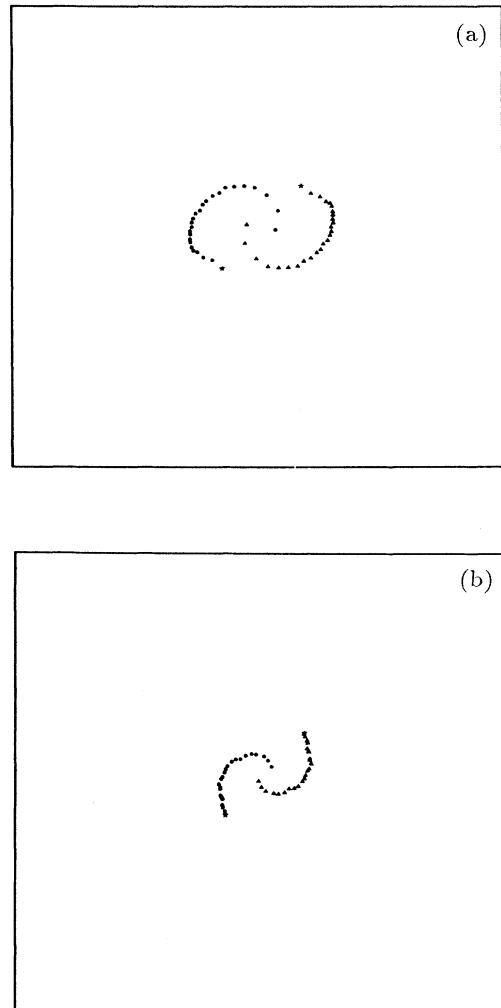

FIG. 7. Same simulation as in Figs. 6(a) and 6(b), but here with $p_1 = -p_2 = 1$; in (b) the time between two successive points is four in our units.

c_3 and c_4 are constants which match the asymptotic out-of-plane solutions at $r = r_v$ [r_v is given by Eq. (2.10)], $\delta = 1 + \lambda$, and the functions $f(r,v)$ and $g(r,v)$ are given by Eqs. (A10) and (A12). At the beginning of Sec. II, we observed that the magnetization field **M** in (2.1) could be expressed through the spin field. Here we have to average over both sublattices to get the appropriate field.

We will now discuss the two different λ regimes ($\lambda < \lambda_c$ and $\lambda > \lambda_c$) separately. In the out-of-plane case [Eq. (4.3)] the even and odd spins are perfectly antialigned in the static case (the same is true for the in-plane case—see below) and the resulting magnetization field is therefore exactly zero. Though even and odd spins are located at different lattice sites, in the continuum limit we have angle fields which are defined on the whole plane for each sublattice. For this reason we are able to calculate an average at every coordinate **r** of the plane. The small deviations from the static structure due to the motion do not contribute to the gyrovector, but give a finite, velocity-dependent dissipation. Thus, from the three terms in Eq. (2.2), only the dissipation term and the static force remain, which causes pure repulsion or attraction depending on whether we consider two vortices with equal q's [Fig. 8(a)] or a vortex and an antivortex (Fig. 9). For the simulations with equal q's, we used the initial positions from Eq. (3.1), while for the other simulation we started with initial positions

$$(x_1, y_1) = (18.5, 18.5) \quad \text{(vortex)},$$
$$(x_2, y_2) = (32.5, 33.5) \quad \text{(antivortex)}. \tag{4.4}$$

The time between two following points for all these simulations (Figs. 8–10) is four in our units. The asymmetry in the velocities of the two vortices in Fig. 8(a) is caused by an additional vortex, which is pinned at (46.5,49.5). Figure 8(b) shows the averaged out-of-plane components of the four spins around the vortex core. As expected, this quantity is zero on the average. The fluctuations around this value are due to the discrete lattice: If the vortex core is not exactly in the middle of a plaquette, then the four spins, which contribute to qn, have different distances to the core and therefore have slightly different z components.

For $\lambda < \lambda_c$ the in-plane angles describe a perfect antiferromagnetic structure, which yields a vanishing gyrovector, but the out-of-plane angles show the same behavior as in the ferromagnetic case: On one side of the direction of motion, all the spins point above, and on the other side all the spins point below the xy plane. The magnitude of these components increases with increasing velocity, but decreases if λ becomes larger. This is different from the ferromagnet case. But here the two ferromagnetic domains in the z components of the spins on the left and right sides of the direction of motion will be less favorable for the system because they will increase the energy, which depends on the magnitude of S_z and λ.

The trajectories of two vortices for $\lambda < \lambda_c$ (Fig. 10, equal q's) is very similar to the equivalent ferromagnetic case: (1) the vortices move on straight lines with small deviations due to the discreteness of the lattice; (2) the motion will stop after a short time, because the force be-
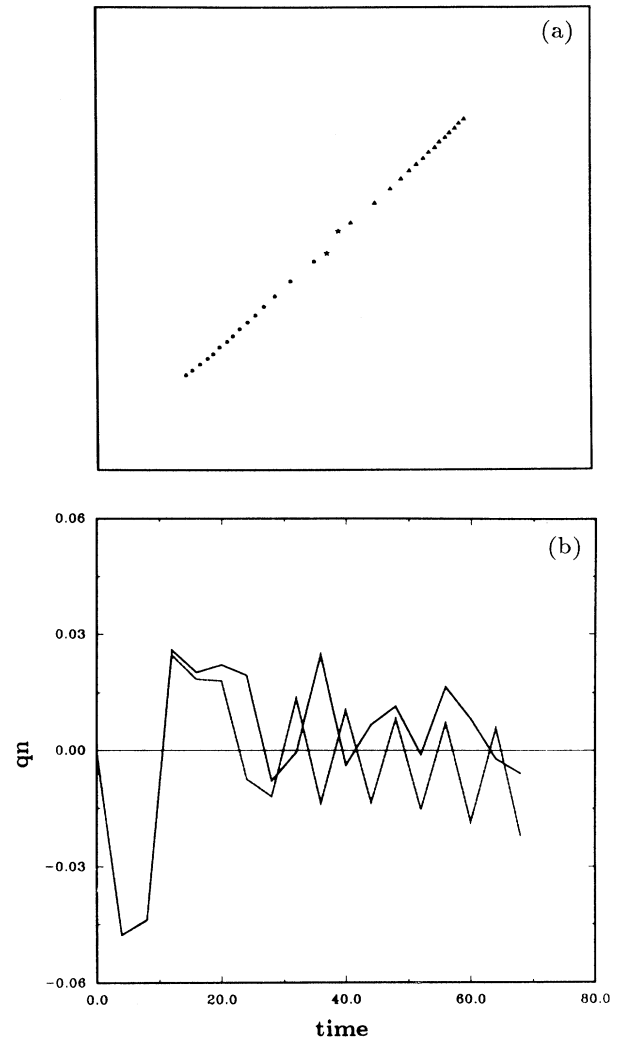

FIG. 8. Vortex-vortex ($q_1 = q_2 = 1$) simulations on an antiferromagnet with $\lambda = 0.9$ and initialized with two static in-plane vortices: (a) trajectories and (b) qn vs time.
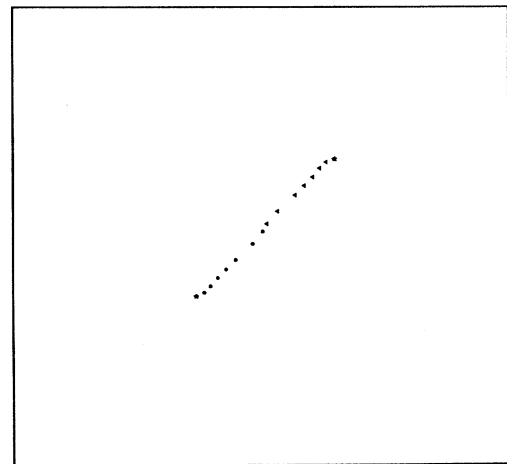

FIG. 9. Vortex-antivortex ($q_1 = -q_2 = 1$) simulation on an antiferromagnet with parameters as in Fig. 8.
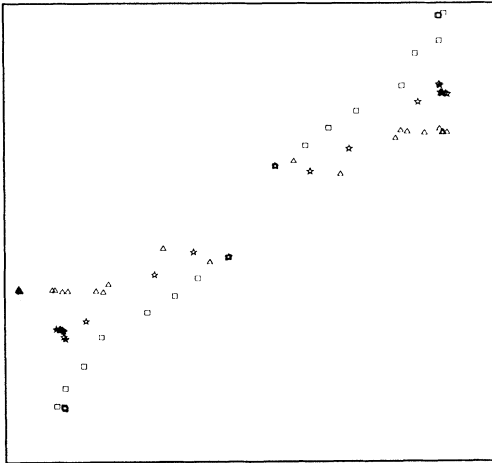
FIG. 10. Vortex-vortex simulations analogous to Fig. 4, but for an antiferromagnet.

tween them becomes too weak beyond some distance to overcome the discreteness potential. Because the antiferromagnetic vortices move (almost) on straight lines for both $\lambda < \lambda_c$ and $\lambda > \lambda_c$, it is not possible to observe whether there is a change in the structure for the fast-moving vortex with $\lambda = 0.6$ (Fig. 10) contrary to the ferromagnetic case (see discussion in Sec. III).

V. CONCLUSION

In the present paper we discussed in detail the dynamics of vortex pairs in XY-spin-symmetry magnetic materials using both analytical and numerical methods. In the analytical part we used an ansatz introduced by Thiele[8] to obtain an effective equation of motion for the center of mass of a single vortex in the presence of other vortices.

Below a critical value λ_c of the anisotropy parameter λ, the vortices are almost in-plane ($\lambda_c \approx 0.72$ for the ferromagnetic and $\lambda_c \approx 0.71$ for the antiferromagnetic 50×50 square lattice). This structure is responsible (i) for an attraction or repulsion of the vortices depending on whether the product of the two vorticities $q_1 q_2$ is positive or negative, respectively, and (ii) for a damping of the motion which is proportional to the logarithm of the vortex radius. The out-of-plane components which are due to the velocity give a small contribution to the damping, but do not change the form of the trajectories. This behavior is true for both ferromagnets and antiferromagnets.

For $\lambda > \lambda_c$ we also find attraction (repulsion) and damping depending on whether $q_1 q_2 < 0$ (> 0), but there is now also the out-of-plane structure which yields different results for the ferromagnet and antiferromagnet. In the ferromagnetic case the z components of the spins around the vortex centers act like an effective magnetic field on the other vortex and vice versa. Now the vortices rotate around each other or move parallel to each other depending on whether $p_1 q_1 = p_2 q_2$ or $p_1 q_1 = -p_2 q_2$, respectively (p carries the sign of the out-of-plane structure). For the antiferromagnet the antialignment of the spins in the two sublattices does not produce an effective

field, and we find no velocity component perpendicular to the line connecting the vortices.

All these features can be seen in our molecular-dynamics simulations. However, in contrast to the analytical work which was done in the continuum limit, we see here, for $\lambda < \lambda_c$, strong discreteness effects of the lattice: The trajectories of the vortices are no longer straight lines (the centers of the vortices try to avoid lattice sites), and for a certain distance the lattice pinning is stronger than the force between the vortices. For $\lambda > \lambda_c$ the out-of-plane structure which is extended over several lattice constants and which yields a ferromagnetic alignment of the S^z components makes the vortices less sensitive to the discreteness effects.

We restricted our analytical investigation here to vortices with a fixed shape which can be described by one collective variable (the "center-of-mass" coordinate). This ansatz is good so long as the density of free vortices is small and the vortex velocity is almost constant—both of these restrictions apply to the $\lambda > \lambda_c$ regime (out-of-plane vortices), where the agreement between analytical and numerical results are very good. But also for $\lambda < \lambda_c$ we obtain quite a good feeling for the vortex motion. A next step to an even better understanding of vortex dynamics is to introduce additional collective variables which also allow a change of the vortex shape—this extension is in preparation.

APPENDIX: EQUATIONS OF MOTION AND VORTEX SOLUTIONS FOR THE ANTIFERROMAGNET

To derive the equations of motion from Eq. (1.1) in the antiferromagnetic case for the continuum limit, we start with the following ansatz for the spins:

$$\mathbf{S}^{\text{even}} = (x \cos\alpha, x \sin\alpha, m) , \tag{A1a}$$

$$\mathbf{S}^{\text{odd}} = (y \cos\beta, y \sin\beta, n) , \tag{A1b}$$

where even and odd denote the two different sublattices, (α, m) and (β, n) are pairs of canonical conjugate variables, and

$$x = (1 - m^2)^{1/2} ,$$

$$y = (1 - n^2)^{1/2} .$$

The equations of motion then are simply given by [H is the Hamiltonian defined in Eq. (1.1)]

$$\dot{\alpha} = \frac{\partial H}{\partial m} , \tag{A2a}$$

$$\dot{m} = -\frac{\partial H}{\partial \alpha} , \tag{A2b}$$

$$\dot{\beta} = \frac{\partial H}{\partial n} , \tag{A2c}$$

$$\dot{n} = -\frac{\partial H}{\partial \beta} , \tag{A2d}$$

or, if we use the variables introduced in Eq. (4.1), by

$$\dot{\Phi}=\tfrac{1}{2}(\dot{\alpha}+\dot{\beta})$$

$$=\tfrac{1}{2}JS\{4\cos2\phi[\tan(\Theta+\theta)\cos(\Theta-\theta)-\tan(\Theta-\theta)\cos(\Theta+\theta)]+8\lambda\sin\theta\cos\Theta+2\lambda\Delta(\sin\theta\cos\Theta)$$

$$+\tan(\Theta+\theta)[\sin2\phi[\Delta(\Phi-\phi)\cos(\Theta-\theta)=2\,\mathrm{grad}(\Phi-\phi)\mathrm{grad}(\Theta-\theta)\sin(\Theta-\theta)]$$

$$-\cos2\phi(\{[\mathrm{grad}(\Phi-\phi)]^2+[\mathrm{grad}(\Theta-\theta)]^2\}\cos(\Theta-\theta)+\Delta(\Theta-\theta)\sin(\Theta-\theta))]$$

$$-\tan(\Theta-\theta)[\sin2\phi[-\Delta(\Phi+\phi)\cos(\Theta+\theta)+2\,\mathrm{grad}(\Phi+\phi)\mathrm{grad}(\Theta+\theta)\sin(\Theta+\theta)]$$

$$-\cos2\phi(\{[\mathrm{grad}(\Phi+\phi)]^2+[\mathrm{grad}(\Theta+\theta)]^2\}\cos(\Theta+\theta)+\Delta(\Theta+\theta)\sin(\Theta+\theta))]\}\ ,\qquad\text{(A3a)}$$

$$\dot{\phi}=\tfrac{1}{2}(\dot{\alpha}-\dot{\beta})$$

$$=\tfrac{1}{2}JS\{4\cos2\phi[\tan(\Theta+\theta)\cos(\Theta-\theta)+\tan(\Theta-\theta)\cos(\Theta+\theta)]-8\lambda\sin\Theta\cos\theta-2\lambda\Delta(\sin\Theta\cos\theta)$$

$$+\tan(\Theta+\theta)[\sin2\phi[\Delta(\Phi-\phi)\cos(\Theta-\theta)-2\,\mathrm{grad}(\Phi-\phi)\mathrm{grad}(\Theta-\theta)\sin(\Theta-\theta)]$$

$$-\cos2\phi(\{[\mathrm{grad}(\Phi-\phi)]^2+[\mathrm{grad}(\Theta-\theta)]^2\}\cos(\Theta-\theta)+\Delta(\Theta-\theta)\sin(\Theta-\theta))]$$

$$+\tan(\Theta-\theta)[\sin2\phi[-\Delta(\Phi+\phi)\cos(\Theta+\theta)+2\,\mathrm{grad}(\Phi+\phi)\mathrm{grad}(\Theta+\theta)\sin(\Theta+\theta)]$$

$$-\cos2\phi(\{[\mathrm{grad}(\Phi+\phi)]^2+[\mathrm{grad}(\Theta+\theta)]^2\}\cos(\Theta+\theta)+\Delta(\Theta+\theta)\sin(\Theta+\theta))]\}\ ,\qquad\text{(A3b)}$$

$$\dot{\Theta}=\frac{1}{2}\left[\frac{\dot{m}}{x}+\frac{\dot{n}}{y}\right]$$

$$=\tfrac{1}{2}JS[-8\sin2\phi\cos\Theta\cos\theta+\sin2\phi(\Delta(\Theta-\theta)\sin(\Theta-\theta)+\{[\mathrm{grad}(\Phi-\phi)]^2+[\mathrm{grad}(\Theta-\theta)]^2\}\cos(\Theta-\theta))$$

$$+\cos2\phi[\Delta(\Phi-\phi)\cos(\Theta-\theta)-2\,\mathrm{grad}(\Phi-\phi)\mathrm{grad}(\Theta-\theta)\sin(\Theta-\theta)]$$

$$+\sin2\phi(\Delta(\Theta+\theta)\sin(\Theta+\theta)+\{[\mathrm{grad}(\Phi+\phi)]^2+[\mathrm{grad}(\Theta+\theta)]^2\}\cos(\Theta+\theta))$$

$$+\cos2\phi[-\Delta(\Phi+\phi)\cos(\Theta+\theta)+2\,\mathrm{grad}(\Phi+\phi)\mathrm{grad}(\Theta+\theta)\sin(\Theta+\theta)]]\ ,\qquad\text{(A3c)}$$

$$\dot{\theta}=\frac{1}{2}\left[\frac{\dot{m}}{x}-\frac{\dot{n}}{y}\right]$$

$$=\tfrac{1}{2}JS[-8\sin2\phi\sin\Theta\sin\theta+\sin2\phi(\Delta(\Theta-\theta)\sin(\Theta-\theta)+\{[\mathrm{grad}(\Phi-\phi)]^2+[\mathrm{grad}(\Theta-\theta)]^2\}\cos(\Theta-\theta))$$

$$+\cos2\phi[\Delta(\Phi-\phi)\cos(\Theta-\theta)-2\,\mathrm{grad}(\Phi-\phi)\mathrm{grad}(\Theta-\theta)\sin(\Theta-\theta)]$$

$$-\sin2\phi(\Delta(\Theta+\theta)\sin(\Theta+\theta)+\{[\mathrm{grad}(\Phi+\phi)]^2+[\mathrm{grad}(\Theta+\theta)]^2\}\cos(\Theta+\theta))$$

$$-\cos2\phi[-\Delta(\Phi+\phi)\cos(\Theta+\theta)+2\,\mathrm{grad}(\Phi+\phi)\mathrm{grad}(\Theta+\theta)\sin(\Theta+\theta)]]\ .\qquad\text{(A3d)}$$

As in the ferromagnetic case,[5,6] we first look for static solutions. We furthermore make the assumption that here the static vortex solutions are only described by the capital angles Φ and Θ, because a local perfect antiferromagnetic structure (which results from this assumption) should give minimal energy in the continuum limit. With these considerations Eqs. (A3) reduce to

$$\cos\Theta\Delta\Phi-2(\mathrm{grad}\Phi)(\mathrm{grad}\Theta)\sin\Theta=0\ ,\qquad\text{(A4a)}$$

$$\frac{\sin^2\Theta+\lambda\cos^2\Theta}{\cos\Theta}\Delta\Theta+(1-\lambda)\sin\Theta(\mathrm{grad}\Theta)^2$$

$$-[4(1-\lambda)-(\mathrm{grad}\Phi)^2]\sin\Theta=0\ .\qquad\text{(A4b)}$$

Equations (A4) have a pure in-plane solution,

$$\Phi(\mathbf{r})=q\arctan\frac{y}{x}+\Phi_c\ ,\qquad\text{(A5)}$$

$$\Theta(\mathbf{r})=0\ ,$$

and an out-of-plane solution,

$$\Phi(\mathbf{r})=q\arctan\frac{y}{x}+\Phi_c\ ,\qquad\text{(A6)}$$

$$\Theta(\mathbf{r})\sim\begin{cases}c_3 r/r_v & \text{as }r\to0\ ,\\ \pi/2-c_4\sqrt{(r_v/r)}\,e^{-r/r_v} & \text{as }r\to\infty\ .\end{cases}$$

A numerical stability analysis shows that the vortex solution (A5) is stable for all $\lambda<\lambda_c$ and the solution (A6) is stable for $\lambda>\lambda_c$ with $\lambda_c\approx0.71$ on a 50×50 square lattice (if the vortex core is in the middle of a plaquette of four

spins, then the discrete solution is, because of the high symmetry, comparable to the continuum solution).

To calculate the change of the vortex shapes due to a small motion, we insert the static solutions (A5) and (A6) in Eq. (A3) and expand to first order in the velocity. For $\lambda < \lambda_c$ (in-plane vortex) only one of the four differential equations becomes velocity dependent:

$$\lambda \Delta \theta + \left[4(1+\lambda) - \left[\frac{q}{r} \right]^2 \right] \theta = \frac{vq}{JS} \frac{\sin(\varphi - \epsilon)}{r} , \quad (A7)$$

and we obtain

$$\theta(r,\varphi) \sim \begin{cases} \dfrac{v}{qJS} r \sin(\varphi - \epsilon) & \text{as } r \to 0 , \\[2ex] -\dfrac{qv}{4(1+\lambda)JS} \dfrac{\sin(\varphi - \epsilon)}{r} & \text{as } r \to \infty , \end{cases} \quad (A8)$$

while Φ, Θ, and ϕ are no functions of the velocity in this linear approximation; ϵ is the angle between the x axis and the direction of motion. The vortex develops out-of-plane components which point on one side of the line of motion above on the other side below the plane. A similar solution was found for the ferromagnet,[6] but there the denominator in (A8) for the large-r limit contains a factor $(1-\lambda)$ instead of $(1+\lambda)$.

For the out-of-plane vortex and for large r, we obtain two velocity-dependent differential equations: one for the angle θ, which has the same form than Eq. (A7) with the large-r solution of (A8), the other for the angle ϕ,

$$\Delta \phi + [8 - (\text{grad}\Phi)^2]\phi = \frac{v}{JS}(\partial_r \Theta)\cos(\varphi - \epsilon) , \quad (A9)$$

with the solution

$$\phi = \frac{vc_4}{JS} \frac{r_v}{8r_v^2 + 1} \cos(\varphi - \epsilon) \left[\frac{r_v}{r} \right]^{1/2} e^{-r/r_v} \left[1 + o\left[\frac{r_v}{r} \right] \right] . \quad (A10)$$

For small r we obtain two coupled differential equations from (A3), viz.,

$$-\frac{vq}{JS}\frac{\sin(\varphi - \epsilon)}{r}\Theta^2 - 2(\text{grad}\Phi)(\text{grad}\phi)\Theta^2$$

$$= \{8\Theta + 4\lambda\Theta^3 - [(\text{grad}\Phi)^2 + (\text{grad}\Theta)^2]2\Theta - \Delta\Theta\}\theta - 2(\text{grad}\Theta)(\text{grad}\theta)\Theta^2 - \Theta\Delta\theta , \quad (A11a)$$

and

$$-\frac{v}{JS}(\partial_r \Theta)\cos(\varphi - \epsilon) - 2(\text{grad}\Phi)(\text{grad}\theta) = \{-8\Theta + [(\text{grad}\Phi)^2 + (\text{grad}\Theta)^2]2\Theta - \Delta\Theta\}\phi - 2(\text{grad}\Theta)(\text{grad}\phi) - \Theta\Delta\phi . \quad (A11b)$$

In lowest order in r, the solutions of (A11) are

$$\phi(\mathbf{r}) = \frac{v}{JS}\frac{5 + 2q^2}{35 + 4q^2} r \cos(\varphi - \epsilon), \quad \theta(\mathbf{r}) = \frac{5vqc_3}{JSr_v(35 + 4q^2)} r^2 \sin(\varphi - \epsilon) . \quad (A12)$$

*Permanent address: Physics Institute, University of Bayreuth, D-8580 Bayreuth, Federal Republic of Germany.

†Permanent address: Physics Department, Kansas State University, Manhattan, Kansas 66506.

[1] K. Hirakawa, H. Yoshizawa, and K. Ubukoshi, J. Phys. Soc. Jpn. 51, 2151 (1982); S. T. Bramwell, M. T. Hutchings, J. Norman, R. Pynn, and P. Day, J. Phys. C 8, 1435 (1988); M. Ain, J. Phys. (Paris) 48, 2103 (1987); L. P. Regnault, J. P. Boucher, J. Rossat-Mignot, J. Bouillot, R. Pynn, J. Y. Henry, and J. P. Renard, Physica B+C 136B, 329 (1986); L. P. Regnault, C. Lartigue, J. F. Legrand, B. Farago, J. Rossat-Mignod, and J. Y. Henry (unpublished).

[2] D. G. Wiesler, H. Zabel, and S. M. Shapiro (unpublished).

[3] M. Pomerantz, Surf. Sci. 142, 556 (1984); D. I. Head, B. H. Blott, and D. Melville, J. Phys. C 8, 1649 (1988).

[4] J. M. Kosterlitz and D. J. Thouless, J. Phys. C 6, 1181 (1973); J. M. Kosterlitz, ibid. 7, 1046 (1974).

[5] F. G. Mertens, A. R. Bishop, G. M. Wysin, and C. Kawabata, Phys. Rev. B 39, 591 (1989).

[6] M. E. Gouvêa, G. M. Wysin, A. R. Bishop, and F. G. Mertens, Phys. Rev. B 39, 11 840 (1989).

[7] A. R. Völkel, G. Wysin, A. R. Bishop, and F. G. Mertens (unpublished).

[8] A. A. Thiele, Phys. Rev. Lett. 30, 230 (1973).

[9] D. L. Huber, Phys. Rev. B 26, 3758 (1982).

[10] V. L. Pokrovsky, M. V. Feigl'man, and A. M. Tsvelick, in Spin Waves and Magnetic Excitations, edited by A. S. Borovik-Romanov, and S. K. Sinha (Elsevier, New York, 1988), Chap. II.

[11] H. M. Wu, E. A. Overman II, and N. J. Zabusky, J. Comput. Phys. 53, 42 (1984).

[12] I. Halperin and D. R. Nelson, J. Low Temp. Phys. 36, 599 (1979).

[13] V. Ambegaokar, B. I. Halperin, D. R. Nelson, and E. G. Siggia, Phys. Rev. B 21, 1806 (1980); W. J. Glaberson and R. J. Donnelly, in Progress in Low Temperature Physics, edited by

D. F. Brewer (Elsevier, New York, 1986), Vol. IX.

[14]A. A. Belavin and A. M. Polyakov, Pis'ma Zh. Eksp. Teor. Fiz. **22**, 503 (1975) [JETP Lett. **22**, 245 (1975)].

[15]Recent calculations (V. L. Pokrovskii and D. V. Khveshchenko, Fiz. Nizk. Temp. **14**, 385 (1988) [Sov. Low Temp. Phys. **14**, 213 (1988)] and references therein) show for a slightly different model than ours that the damping parameter for free vortices just above T_{KT} is $\alpha \approx 0.1(T/T_{KT})^2$.

[16]A. R. Völkel, A. R. Bishop, and F. G. Mertens (unpublished).

[17]J. Friedel, *Dislocations* (Pergamon, Oxford, 1964).

[18]H. J. Mikeska, J. Phys. C **13**, 2913 (1980).